Int. J. Solids Structures Vol. 29, No. 14/15, pp. 1789–1812, 1992
Printed in Great Britain.

0020–7683/92 $5.00 + .00
Pergamon Press plc

THERMAL CRACKING OF TWO-PHASE COMPOSITE STRUCTURES UNDER UNIFORM AND NON-UNIFORM TEMPERATURE DISTRIBUTIONS

K. P. HERRMANN and M. DONG
Laboratorium für Technische Mechanik, Paderborn University, W-4790 Paderborn, Pohlweg 47-49, Federal Republic of Germany

Abstract—In this paper curved thermal crack growth in self-stressed brittle solids subjected to well-defined temperature fields has been studied. The resulting boundary-value problems of the stationary plane thermoelasticity are solved by means of the finite element method. Moreover, by applying an appropriate crack growth criterion based on the total energy release rate of a quasistatic mixed-mode crack extension the further development of thermal crack paths starting at the external surfaces of disk-like two-phase compounds with circular cross-sections could be predicted. Several specimen geometries consisting of different material combinations have been investigated by considering uniform temperature changes and by applying the relevant methods of fracture mechanics. Further, the corresponding fracture mechanical data like strain energy release rates and stress intensity factors, respectively, have been determined by additional considerations of the influence of inner stress concentrators onto the paths of quasistatic extending thermal cracks. The comparison of those theoretical investigations with associated cooling experiments shows a satisfying agreement. Finally, the influences of additional local temperature changes onto the prospective thermal crack paths have been studied by means of the fracture criterion mentioned already as well as by using the finite element method. Thereby the numerical results have shown some remarkable effects of interference between the local temperature changes located in the vicinity of thermal crack tips and the further crack paths.

1. INTRODUCTION

The crack path prediction of extending thermal cracks in dependence on the geometrical configuration of a self-stressed nonhomogeneous solid, as well as of the applied thermal loading, poses an interesting problem in today's fracture mechanics research. There exists experimental evidence for the appearance of different failure mechanisms in thermally loaded composite structures, like curvilinear matrix and interface cracks, respectively, where these thermal cracks arise mostly under mixed-mode loading conditions. Therefore, the study of thermal crack growth in nonhomogeneous materials is necessary for the assessment of the strength of composite structures because modern composite materials are often subjected to variable temperature fields, for example in aircraft and space travel technology. Moreover, from the fracture mechanical standpoint curved or kinked cracks were studied in the past by several authors either as interface cracks along circular inclusions (England, 1966; Toya, 1974; Herrmann, 1983), or in connection with the assessment of existing crack propagation criteria (Cotterell and Rice, 1980; Bergkvist and Guex, 1979; Nemat-Nasser, 1980; Palaniswamy and Knauss, 1978). Furthermore, Piva and Viola (1980) gave a comprehensive survey of the state-of-the-art concerning the interface crack problem, discussing also the cancellation of the oscillatory anomalies of the elastic stress and displacement fields near the tip of an interface crack as well as the establishment of an appropriate crack propagation criterion.

The thermal interface crack problem was studied in the past for example by Brown and Erdogan (1968), Bregman and Kassir (1974), and Srivastava *et al.* (1977). These authors considered two semi-infinite elastic solids with different thermoelastic material properties and having a crack situated along the interface. Further, circular cracks in the interfaces of bounded thermally loaded fibrous composites were investigated by Herrmann and Strathmeier (1983) and Herrmann and Ferber (1989). In addition, curved thermal cracks in glasses have been studied in the past by Hieke (1960), Hieke and Loges (1966), Blauel (1970), and Karihaloo and Nemat-Nasser (1981). Finally, the crack path prediction

of extending thermal cracks in self-stressed glassy compounds in dependence on the geometrical configuration as well as on the applied thermal loading has been considered in several papers by Herrmann and Grebner (1982, 1984a, 1985) and Herrmann and Dong (1990).

In this paper, curvilinear thermal cracks are considered extending in disk-like two-phase compounds due to well-defined thermal stress fields caused by either uniform or non-uniform temperature changes. The cross-sections of several two-phase solids consisting of homogeneous, isotropic and linearly elastic materials with different thermoelastic properties varying discontinuously at the straight interface Γ from the values $E^{(I)}$, $\nu^{(I)}$, $\alpha^{(I)}$ of the region I to the values $E^{(II)}$, $\nu^{(II)}$, $\alpha^{(II)}$ of the region II (E, Young's modulus; ν, Poisson's ratio; α, linear coefficient of thermal expansion), and are shown in Fig. 1 together with the corresponding geometrical parameters. Further, the associated thermoelastic material properties of the two-phase compounds from Fig. 1 are listed in Table 1.

Cooling experiments were performed for a variety of glassy compounds (Grebner, 1983) and other two-phase composite structures showing the initiation and extension of thermal cracks for certain material combinations. Those experiments gave crack paths following in a reasonable agreement special principal stress trajectories belong to the existing thermal stress fields in the associated uncracked two-phase solids. The temporal development of thermal stress fields in the associated uncracked two-phase solids. The temporal development of thermal crack growth in different-shaped two-phase glassy compounds glued together at a temperature near the transformation point of the optical glasses and afterwards subjected to a steady cooling process has been discussed in some detail in a review article by Herrmann (1987).

In this paper, additional theoretical and experimental results are given concerning the initiation and extension of curvilinear thermal cracks in self-stressed metal/glass, plastic/glass and plastic/plastic bimaterial specimens. Thereby an appropriate crack growth

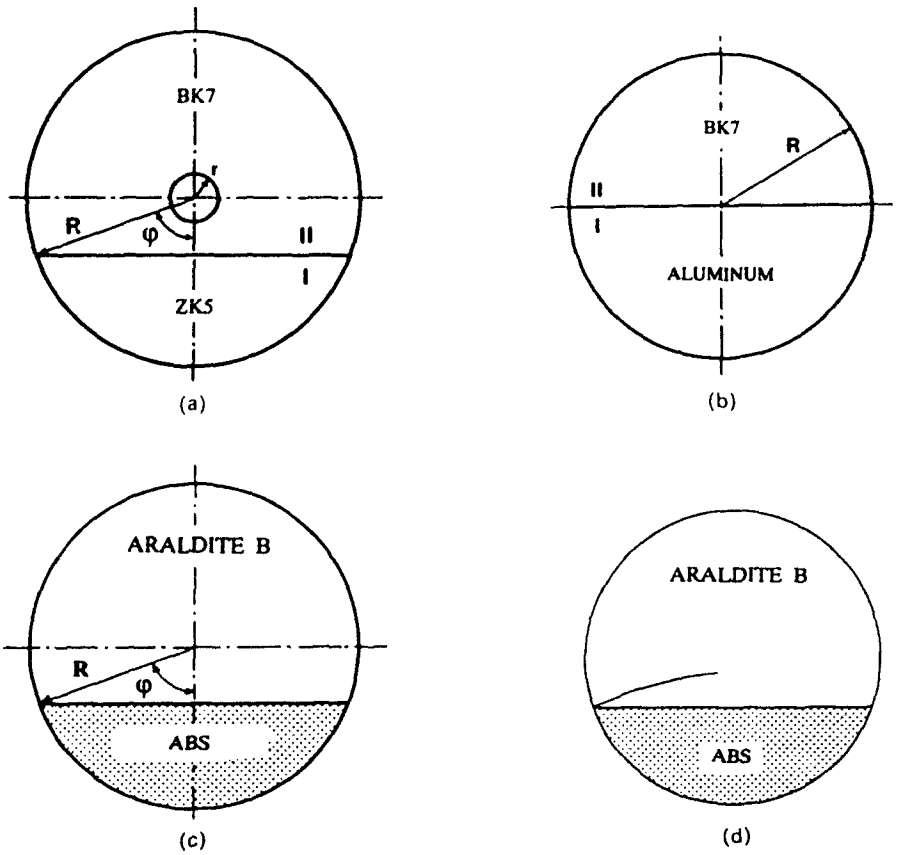

Fig. 1(a)–(d). Cross-sections of disk-like two-phase composite structures.

Table 1. Material properties of the components of two-phase composite structures

Material	BK7 (Glass)	ZK5 (Glass)	PL-1 (Plastic)	Aluminum	ABS (Plastic)	Araldite B
Young's modulus E [Nmm^{-2}]	80148	68180	2880	72000	3000	3500
Poisson's ratio ν [1]	0.211	0.241	0.360	0.340	0.350	0.370
Linear coefficient of thermal expansion α [10^{-6} K^{-1}]	7.1	8.7	70.0	23.9	95.0	45.0

criterion has been established and applied for the prediction of the further development of thermal cracks initiated in these self-stressed two-phase compounds. Besides, the influence of a nonuniform temperature distribution (produced by additional local temperature changes) onto those thermal crack paths has been studied in some detail.

2. FORMULATION AND SOLUTION OF BOUNDARY-VALUE PROBLEMS FOR UNCRACKED AND CRACKED DISSIMILAR MATERIALS

2.1. *Principal stress trajectories in thermally loaded two-phase solids*

The determination of fracture mechanical data governing the quasistatic growth of a curvilinear thermal crack lying in one of the segments of a self-stressed two-phase compound has been performed by applying the concepts of linear elastic fracture mechanics. By assuming the existence of a plane stress state in the cracked composite structure as well as temperature-independent thermoelastic material properties $E^{(J)}$, $\nu^{(J)}$, $\alpha^{(J)}$, $(J = I, II)$, the following mixed boundary-value problem of the plane thermoelasticity has to be solved:

$$\sigma_{ij,j}^{(J)} = 0 \tag{1}$$

$$\sigma_{ij}^{(J)} = 2\mu^{(J)}\varepsilon_{ij}^{(J)} + \lambda^{(J)}e^{(J)}\delta_{ij} - (3\lambda^{(J)} + 2\mu^{(J)})\alpha^{(J)}\Delta T^{(J)}\delta_{ij} \tag{2}$$

$$\varepsilon_{ij}^{(J)} = \tfrac{1}{2}(u_{i,j}^{(J)} + u_{j,i}^{(J)}); \quad (i, j = 1, 2), \tag{3}$$

with $\Delta T^{(J)} = T^{(J)} - T_0$; $J = I, II$ where T_0 represents the temperature of the unstressed initial state. Moreover, the boundary conditions

$$\sigma_{ij}^{(J)} n_j = 0; \quad (i, j = 1, 2) \tag{4}$$

have to be fulfilled where $\mathbf{n}$ means the unit normal vector with respect to the external boundary S and to the two crack surfaces $S^+ \cup S^-$, respectively. In addition, the continuity conditions

$$u_i^{(I)} = u_i^{(II)} \tag{5}$$

$$\sigma_{ij}^{(I)} n_j = \sigma_{ij}^{(II)} n_j \tag{6}$$

have to be satisfied at the discontinuity area Γ where in this case $\mathbf{n}$ means the unit normal vector with respect to the material interface Γ.

By introducing Airy's stress function F, the boundary-value problem (1)–(6) can be transformed into a boundary-value problem of the bipotential theory. By making use of Muskhelishvili's method of complex potentials (Muskhelishvili, 1971) a closed-form solution of this boundary-value problem concerning the two-phase composite structures from Fig. 1 with different uniform temperature distributions in both segments *I* and *II* was given for plane strain conditions by Herrmann (1987).

On the contrary, by expressing the formulated mixed boundary-value problem of the plane thermoelasticity [eqns (1)–(6)], in displacements alone one obtains the following governing equations for the thermally loaded two-phase solids:

$$\mu^{(J)}\nabla^2 u_i^{(J)} + (\lambda^{(J)} + \mu^{(J)})e_{,i}^{(J)} - (3\lambda^{(J)} + 2\mu^{(J)})\alpha^{(J)}(\Delta T^{(J)})_{,i} = 0, \tag{7}$$

where $e^{(J)} = u_{i,i}^{(J)}$; $J = I, II$ and with the boundary conditions

$$[\lambda^{(J)}e^{(J)}\delta_{ij} + \mu^{(J)}(u_{i,j}^{(J)} + u_{j,i}^{(J)}) - (3\lambda^{(J)} + 2\mu^{(J)})\alpha^{(J)}\Delta T^{(J)}\delta_{ij}]n_j = 0 \tag{8}$$

and continuity conditions at the material interface Γ

$$u_i^{(I)} = u_i^{(II)} \tag{9}$$

$$[\lambda^{(I)}e^{(I)}\delta_{ij} + \mu^{(I)}(u_{i,j}^{(I)} + u_{j,i}^{(I)}) - (3\lambda^{(I)} + 2\mu^{(I)})\alpha^{(I)}\Delta T^{(I)}\delta_{ij}]n_j$$
$$= [\lambda^{(II)}e^{(II)}\delta_{ij} + \mu^{(II)}(u_{i,j}^{(II)} + u_{j,i}^{(II)}) - (3\lambda^{(II)} + 2\mu^{(II)})\alpha^{(II)}\Delta T^{(II)}\delta_{ij}]n_j, \tag{10}$$

with $(i, j = 1, 2)$.

In the case of a uniform distribution of the temperature changes $\Delta T^{(J)}$ in both regions [eqn. (7)] turns into a simpler form according to

$$\mu^{(J)}\nabla^2 u_i^{(J)} + (\lambda^{(J)} + \mu^{(J)})e_{,i}^{(J)} = 0, \tag{11}$$

with the following definition of the total displacements $u_i^{(J)}$

$$u_i^{(J)} = u_i^{\sigma(J)} + \alpha^{(J)}\Delta T^{(J)}x_i, \tag{12}$$

where $u_i^{\sigma(J)}$ represent the displacements caused by the self-stresses whereas $\alpha^{(J)}\Delta T^{(J)}x_i$ are the displacements caused by the temperature changes $\Delta T^{(J)}$, $J = I, II$.

Moreover, the displacements $u_i^{\sigma(J)}$ obey the following partial differential equation:

$$\mu^{(J)}\nabla^2 u_i^{\sigma(J)} + (\lambda^{(J)} + \mu^{(J)})e_{,i}^{\sigma(J)} = 0. \tag{12a}$$

Further, the self-stresses are simply expressed as follows:

$$\sigma_{ij}^{(J)} = \lambda^{(J)}e^{\sigma(J)}\delta_{ij} + \mu^{(J)}[u_{i,j}^{\sigma(J)} + u_{j,i}^{\sigma(J)}]. \tag{13}$$

Therefore, the boundary and continuity conditions (8)–(10) read

$$[\lambda^{(J)}e^{\sigma(J)}\delta_{ij} + \mu^{(J)}(u_{i,j}^{\sigma(J)} + u_{j,i}^{\sigma(J)})]n_j = 0 \tag{14}$$

$$u_i^{\sigma(I)} - u_i^{\sigma(II)} = [\alpha^{(II)}\Delta T^{(II)} - \alpha^{(I)}\Delta T^{(I)}]x_i \tag{15}$$

$$[\lambda^{(I)}e^{\sigma(I)}\delta_{ij} + \mu^{(I)}(u_{i,j}^{\sigma(I)} + u_{j,i}^{\sigma(I)})]n_j = [\lambda^{(II)}e^{\sigma(II)}\delta_{ij} + \mu^{(II)}(u_{i,j}^{\sigma(II)} + u_{j,i}^{\sigma(II)})]n_j. \tag{16}$$

In accordance with eqn (11) as well as eqns (14)–(16) a series of conclusions can be drawn:

(a) The stresses in both segments I and II, respectively, are directly proportional to $[\alpha^{II}\Delta T^{(II)} - \alpha^{(I)}\Delta T^{(I)}]$. If this difference equals zero then there exist no thermal stresses at all in both segments of a composite structure, although certain linear displacements appear to be corresponding to the free expansion of the compounds.

(b) All different combinations of $\Delta T^{(I)}$ and $\Delta T^{(II)}$ with corresponding values of $[\alpha^{(II)}\Delta T^{(II)} - \alpha^{(I)}\Delta T^{(I)}]$ lead to the same thermal stress fields in the composite structures with the same geometrical configurations and material combinations. For instance, the combinations $\Delta T^{(I)} = \Delta T^{(II)} = \Delta T$ and $\Delta T^{(I)} = 0$, $\Delta T^{(II)} = [\alpha^{(II)} - \alpha^{(I)}]\Delta T/\alpha^{(II)}$ as well as $\Delta T^{(I)} = [\alpha^{(II)} - \alpha^{(I)}]\Delta T/\alpha^{(I)}$, $\Delta T^{(II)} = 0$ correspond to the same thermal stress field. This means that once the thermal stress field in a two-phase solid subjected to a homogeneous

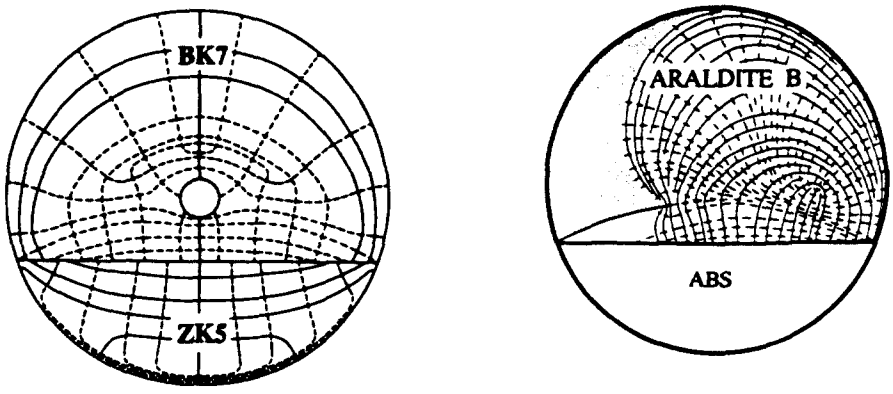

Fig. 2(a) and (b). Principal stress trajectories in the cross-sections of uncracked and cracked self-stressed two-phase composite structures.

temperature field has been determined, then the stresses in the same composite structure under any combinations of two different uniform temperature changes in the two segments are also known.

Moreover, Fig. 2a gives the principal stress trajectories in the circular cross-section of a doubly connected thermally loaded uncracked two-phase composite structure (material combination: BK7 (region *I*)/ZK5 (region *II*)) containing an inner stress concentrator (hole). In this case the geometrical parameters were chosen as $R = 16.5$ mm, $r = R/10$, $\phi = 70°$ and the applied uniform temperature distribution reads $\Delta T^{(I)} = \Delta T^{(II)} = \Delta T = -560°C$.

Thereby the principal stress trajectories of Fig. 2a can be gained by a graphical integration procedure of the following ordinary differential equation:

$$2\sigma_{xy}\,dy + \{(\sigma_{xx} - \sigma_{yy}) \mp \sqrt{(\sigma_{yy} - \sigma_{xx})^2 + 4\sigma_{xy}^2}\}\,dx = 0, \tag{17}$$

where the stress components have been taken from the corresponding solution of the boundary-value problem of the stationary plane thermoelasticity [eqns (1)–(6)]. Furthermore, Fig. 2a shows the existence of two orthogonal sets of principal stress trajectories (solid lines: tension stresses; dotted lines: pressure stresses) which embrace two singular points on the symmetry line of the cross-section.

Further results for thermally loaded glassy compounds with quadratic and hexagonal cross-sections, respectively, have been obtained and can be found in the references (Herrmann, 1987; Herrmann and Grebner, 1984). Besides, a comparison of those theoretically determined self-stress states with corresponding fields of experimental principal stress trajectories in stable uncracked bimaterial specimens (Grebner, 1983; Herrmann and Grebner, 1984) obtained by using the method of photoelasticity showed a very good coincidence. Moreover, the theoretically as well as the experimentally gained fields of principal stress trajectories indicate very clearly that for the cases $2\phi \neq \pi$ only one principal stress trajectory of the two existing sets runs from one intersection point of the interface Γ with the external boundary S to the opposite intersection point. Furthermore, cooling experiments performed for different-shaped bimaterial specimens have indicated that for so-called unstable material combinations a curvilinear thermal crack starts with a special initial velocity from one of the two intersection points and runs with decreasing velocity to the opposite intersection point, thereby using this principal stress trajectory mentioned above as a guide line. Besides, the experimental as well as the theoretical thermal stress fields show for the case $2\phi = \pi$ the existence of two principal stress trajectories (one in each semicircle) running into the two intersection points. But the cooling experiments showed that one crack only arises, starting again from one of the two intersection points. Further results concerning curvilinear thermal crack growth in disk-like two-phase compounds are given in Fig. 6. Finally, Fig.

2b shows the field of principal stress trajectories in the cross-section of a thermally cracked disk-like bimaterial specimen (material combination: ABS (region *I*)/Araldite B (region *II*)). It can be stated that in the case of uniform cooling of an unstable two-phase compound a thermal crack arises on that side of the material interface where Min $[\alpha^{(J)}, J = I, II]$ is valid. Furthermore, the theoretically obtained principal stress trajectories of Fig. 2b were confirmed by corresponding experimental thermal stress fields gained by using the method of photoelasticity (Ferber *et al.*, 1990).

3. CRACK PATH PREDICTION AND CALCULATION OF FRACTURE MECHANICAL DATA CONCERNING THERMAL CRACKS ARISING IN SELF-STRESSED TWO-PHASE SOLIDS SUBJECTED TO UNIFORM TEMPERATURE DISTRIBUTIONS

3.1. *Crack growth criterion*

A theoretical crack path prediction in thermally loaded two-phase composite structures requires the solution of different mixed boundary-value problems of the plane thermoelasticity according to eqns (1)–(6) where the boundary conditions (4) have to be numerically fulfilled at the stress-free boundaries S (external surface) and $S^+ \cup S^-$ (crack surfaces), respectively. Because of the complicated shape of the stress-free boundary of such a cracked two-phase solid, a numerical calculation was performed by applying the finite element method in order to predict the curvilinear crack path by means of an appropriate crack growth criterion. In the past several directional criteria for crack propagation in brittle solids have been proposed, such as the criteria of principal stress (Erdogan and Sih, 1963), minimum of strain energy density (Sih, 1973, 1974), maximum of strain energy release rate (Hussain *et al.*, 1972; Strifors, 1974). Thereby these criteria require the knowledge of the near-tip stress and displacement fields in the vicinity of the original crack tip characterized for a general plane loading situation by the stress intensity factors K_I and K_{II}, respectively. Furthermore, the application of these criteria to a cracked brittle solid delivers equations for the determination of the angle θ describing the direction of further crack growth (cf. Fig. 3). Investigations performed in Bergkvist and Guex (1979) showed in the case of small angles θ the existence of an approximate solution,

$$\theta = -2K_{II}/K_I, \tag{18}$$

valid for all projective crack propagation criteria. Based on this important result finite element calculations were performed concerning the theoretical prediction of a curvilinear thermal crack path in a two-phase glassy compound. Thereby a standard finite element program was used by applying the substructure technique as well as by using triangular linear strain six-node elements. Further, the numerically determined crack path showed a fairly good agreement with experimental results obtained by appropriate cooling experiments (Herrmann, 1987; Herrmann and Grebner, 1984a).

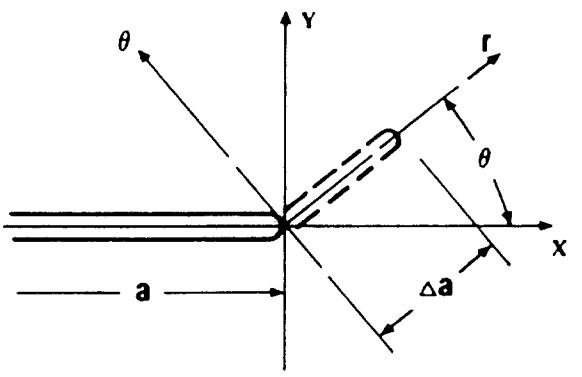

Fig. 3. Global and local coordinates at a kinked crack tip.

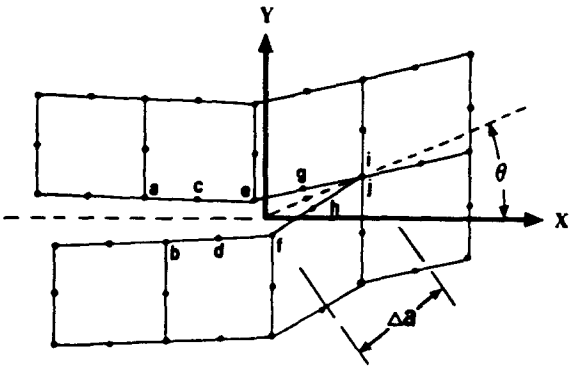

Fig. 4. Finite element mesh and global coordinates at the crack tip with a new crack lengthening Δa.

In this paper, by combining the essentials from the principal stress and the maximum energy release rate criterion, an appropriate crack growth criterion based upon the numerical calculation of energy release rates at crack tips has been proposed. It has been shown already in Herrmann and Grebner (1984a) that the determination of strain energy release rates at the tips of quasistatically extending curvilinear thermal cracks in self-stressed two-phase solids can be performed applying a method described by Rybicki and Kanninen (1977). This method is based on the evaluation of Irwin's crack closure integral:

$$G(a,\theta) = G_I(a,\theta) + G_{II}(a,\theta) = \lim_{\Delta a \to 0} \frac{1}{2\Delta a} \int_0^{\Delta a} [\sigma_{\theta\theta}(r,\theta) \cdot \bar{u}_\theta(r,\theta)]\, dr + \lim_{\Delta a \to 0} \frac{1}{2\Delta a} \int_0^{\Delta a} [\sigma_{r\theta}(r,\theta) \cdot \bar{u}_r(r,\theta)]\, dr. \quad (19)$$

Here the quantities $\sigma_{\theta\theta}$, $\sigma_{r\theta}$ in eqn (19) represent the near-tip stresses in the local coordinate system at the crack tip prior to crack extension, whereas the quantities $\bar{u}_r$, $\bar{u}_\theta$ stand for the corresponding normal and tangential displacements between opposite points of the crack surface after crack extension and Δa represents the crack lengthening. By using a finite element mesh according to Fig. 4 a numerical calculation of the average energy release rates G, G_I, G_{II} related to the global coordinate system x, y as indicated can be performed where the displacements along the new crack surfaces are approximated by a quadratic interpolation function in the related finite elements, i.e. usually 8-node isoparametric or 6-node triangular elements. The corresponding formulae read

$$G_I\left(a+\frac{\Delta a}{2},0\right) \approx G_I(a \to a+\Delta a,0) = A\sin^2\theta - B\sin\theta\cos\theta + C\cos^2\theta \quad (20)$$

$$G_{II}\left(a+\frac{\Delta a}{2},0\right) \approx G_{II}(a \to a+\Delta a,0) = A\cos^2\theta + B\sin\theta\cos\theta + C\sin^2\theta \quad (21)$$

$$G\left(a+\frac{\Delta a}{2},0\right) = G_I\left(a+\frac{\Delta a}{2},0\right) + G_{II}\left(a+\frac{\Delta a}{2},0\right) = A + C \quad (22)$$

with

$$A = \frac{1}{2t\Delta a}[F_x^f(u_x^e - u_x^f) + F_x^h(u_x^g - u_x^h)] \quad (23)$$

$$B = \frac{1}{2t\Delta a}[F_x^f(u_y^e - u_y^f) + F_x^h(u_y^g - u_y^h) + F_y^f(u_x^e - u_x^f) + F_y^h(u_x^g - u_x^h)] \quad (24)$$

$$C = \frac{1}{2t\Delta a}[F_x^f(u_x^e - u_x^f) + F_y^h(u_y^g - u_y^h)] \tag{25}$$

where F_x^i, F_y^i $(i = f, h)$ denote the components of the nodal forces in the global coordinate system x, y before the crack extension Δa, and u_x^i, u_y^i $(i = e, f, g, h)$ stand for the components of the corresponding nodal displacements of the new crack surfaces after crack extension.

Now by applying the eqns (20)–(22) the energy release rates G, G_I, G_{II} can be calculated if the new crack extension direction θ is known. However, only latter quantity is wanted. Therefore, in the following an approximate method for the determination of the new crack propagation direction is proposed, based on the physical mechanism of brittle fracture. Thus, it is assumed that the new direction of crack lengthening Δa is given by the direction in which $G_{II} = 0$ holds true and crack extension occurs for $G_I \geqslant G_{Ic}$ (critical crack extension force). Based upon this criterion and the numerical calculation of the energy release rates G_j $(j = I, II)$ the following iteration scheme concerning the determination of the new crack extension direction could be established.

Step 0: Select a possible direction θ^* of crack propagation

Step 1: Let $\theta = \theta^*$ by means of arranging a local finite element mesh in the vicinity of the crack tip and calculate with this preliminary propagation angle a set of coefficients A, B, C according to eqns (23)–(25) as well as the corresponding values of the energy release rates, eqns (20)–(22). Now, if $G_{II} = 0$ is valid, then θ^* represents already the desired new crack extension direction and the iteration is finished. But G_{II} may not be zero; then one has to add

Step 2: By taking $G_{II} = 0$ it follows that

$$G_{II}(\theta) = A\cos^2\theta + B\sin\theta\cos\theta + C\sin^2\theta = 0. \tag{26}$$

From eqn (26) a new angle θ^* for the desired crack extension direction can be obtained, namely

$$\theta^* = \arctan\left[\frac{-B \pm \sqrt{B^2 - 4AC}}{2C}\right]. \tag{27}$$

If the inequality $4AC > B^2$ is valid, then in case of $A < C$ relation (28) holds true:

$$\theta^* = \tfrac{1}{2}\arctan\left[\frac{B}{A - C}\right]. \tag{28}$$

Equation (28) corresponds to Min $[G_{II}]$ and therefore Max $[G_I]$. Thus, the following relations have to be fulfilled:

$$\frac{\partial G_I}{\partial\theta} = 0, \quad \frac{\partial^2 G_I}{\partial\theta^2} < 0 \tag{29}$$

$$\frac{\partial G_{II}}{\partial\theta} = 0, \quad \frac{\partial^2 G_{II}}{\partial\theta^2} > 0. \tag{30}$$

Further, there exists two other possible cases; namely for $A > C$ and $B > 0$ the following is valid:

$$\theta^* = \tfrac{1}{2}\arctan\left[\frac{B}{A - C}\right] - \frac{\pi}{2} \tag{31}$$

and for $A > C$ and $B < 0$ it follows that

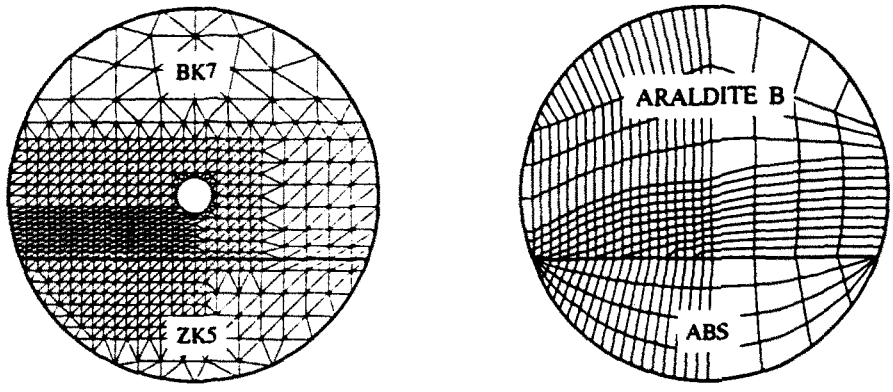

Fig. 5(a) and (b). Finite element meshes used for crack path prediction.

$$\theta^* = \tfrac{1}{2}\arctan\left[\frac{B}{A-C}\right] + \frac{\pi}{2}. \tag{32}$$

After getting this new crack extension direction θ^* a new start of the iteration scheme can be again performed. After a few reiterations of the steps 1 and 2 the procedure can be stopped if the new angle θ^* nearly equals θ, the former used to calculate the coefficients A, B, C. Then also the energy release rate G_{II} reaches approximately the value zero, and therefore this calculated angle corresponds to the new crack propagation angle.

3.2. *Thermal crack path prediction in self-stressed two-phase compounds*

This crack growth criterion established in the previous chapter has been used for the prediction of curvilinear thermal crack paths originated in different shaped two-phase

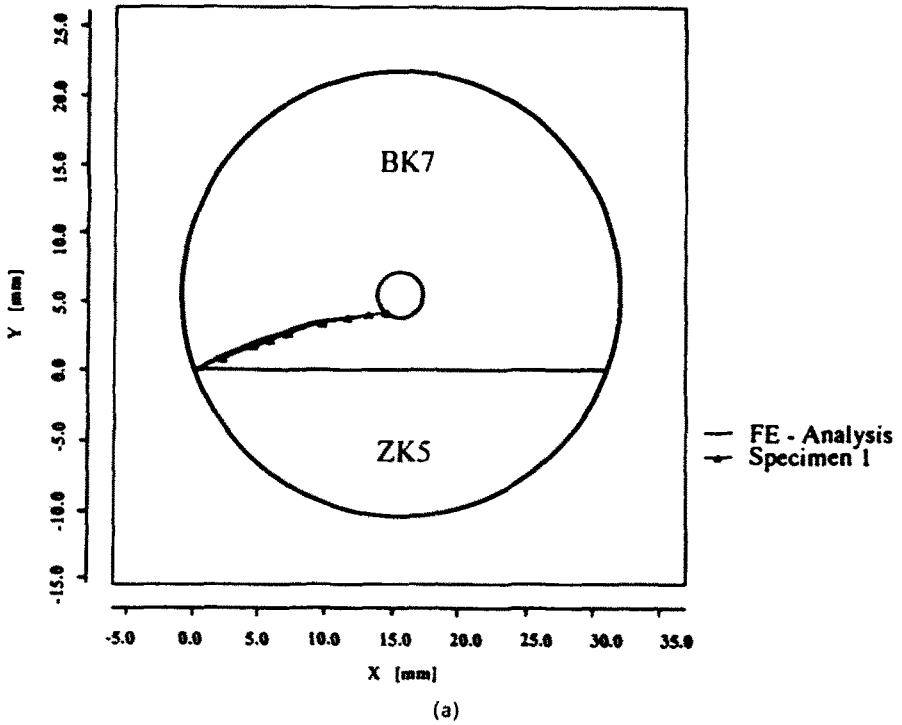

Fig. 6(a). (*continued overleaf*).

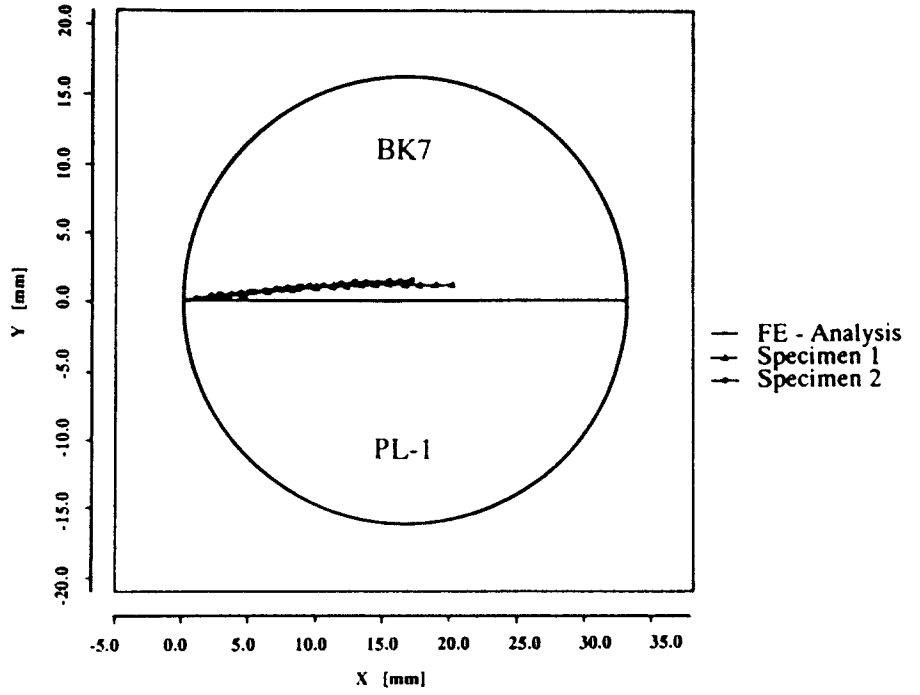
BK7
PL-1
Y [mm]
X [mm]
-5.0
0.0
5.0
10.0
15.0
20.0
25.0
30.0
35.0
-20.0
-15.0
-10.0
-5.0
0.0
5.0
10.0
15.0
20.0
FE - Analysis
Specimen 1
Specimen 2

(b)

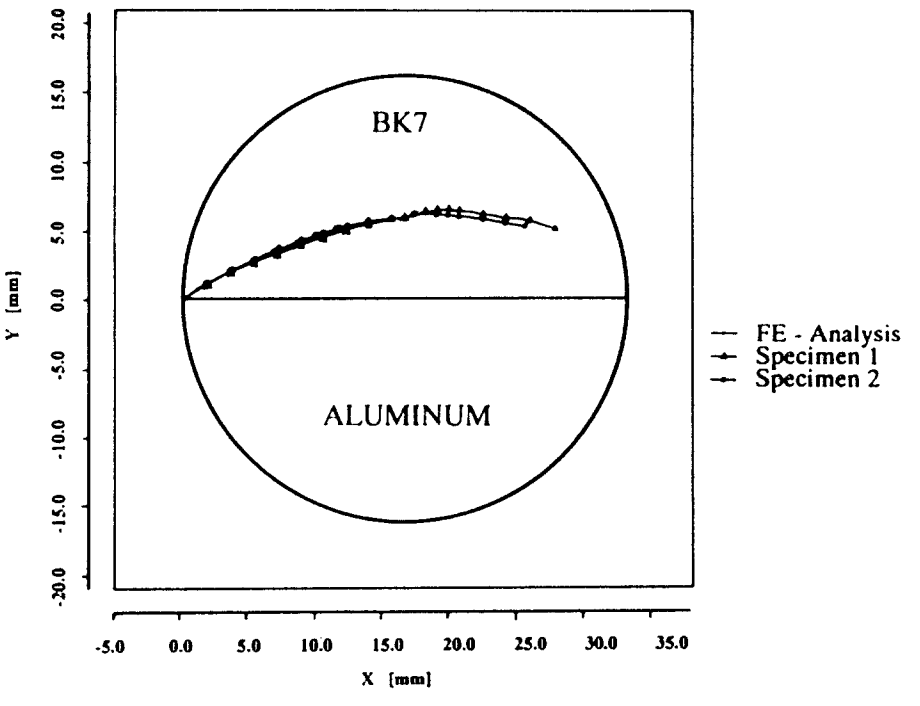
BK7
ALUMINUM
Y [mm]
X [mm]
-5.0
0.0
5.0
10.0
15.0
20.0
25.0
30.0
35.0
-20.0
-15.0
-10.0
-5.0
0.0
5.0
10.0
15.0
20.0
FE - Analysis
Specimen 1
Specimen 2

(c)

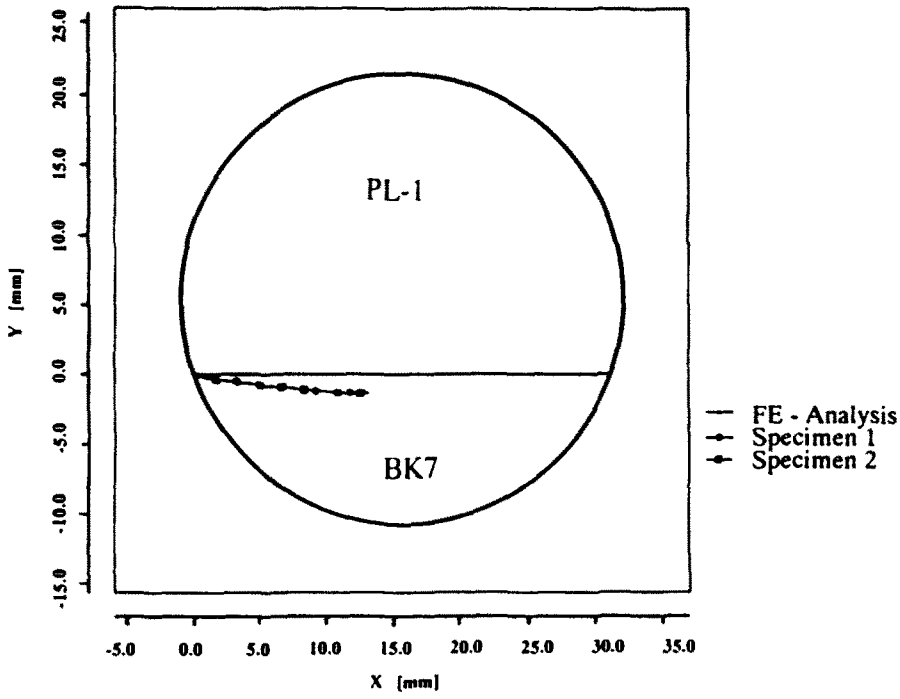

(d)

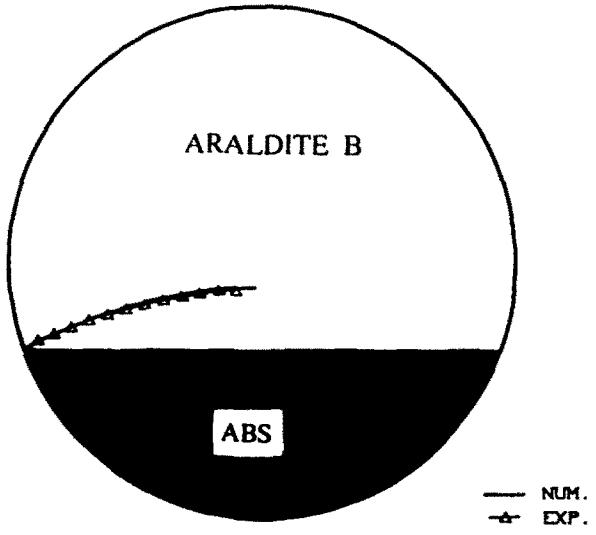

(e)

Fig. 6(a)–(e). Comparison of numerically and experimentally obtained crack paths in different thermally loaded two-phase compounds.

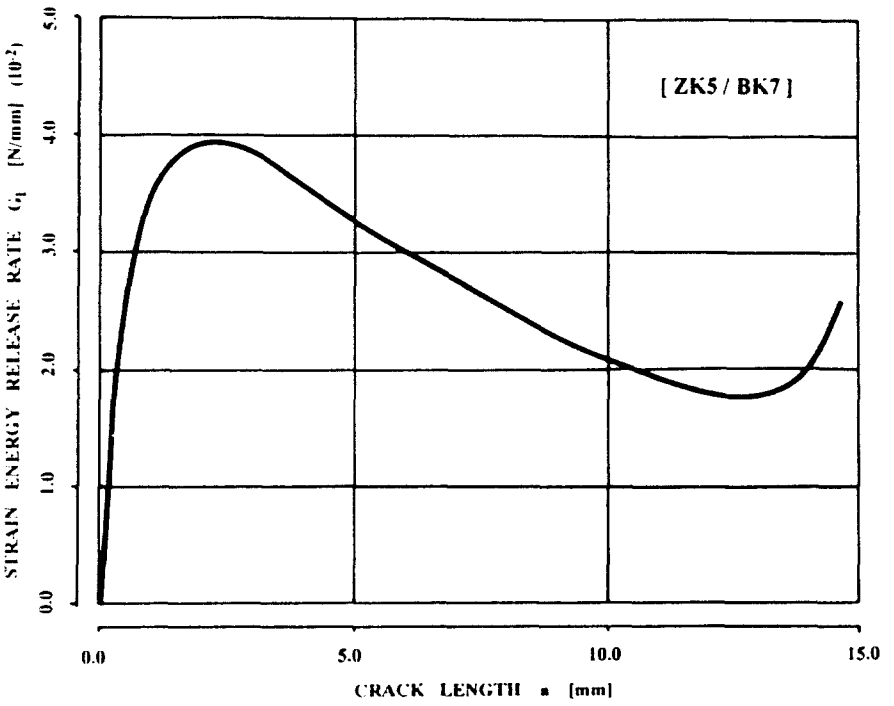
[ZK5 / BK7]
STRAIN ENERGY RELEASE RATE G_I [N/mm] (10^{-2})
0.0
1.0
2.0
3.0
4.0
5.0
0.0
5.0
10.0
15.0
CRACK LENGTH a [mm]

(a)

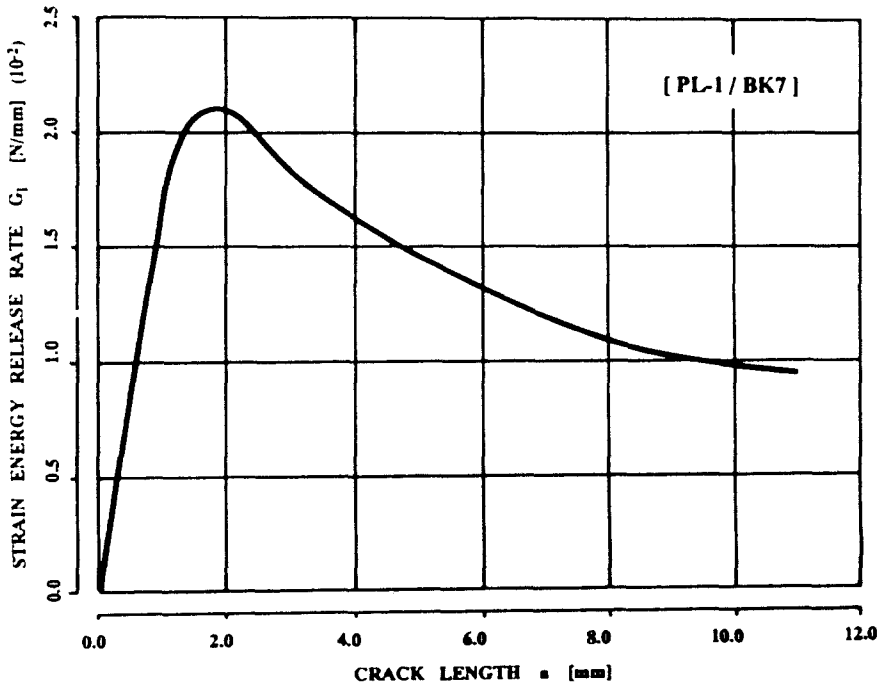
[PL-1 / BK7]
STRAIN ENERGY RELEASE RATE G_I [N/mm] (10^{-2})
0.0
0.5
1.0
1.5
2.0
2.5
0.0
2.0
4.0
6.0
8.0
10.0
12.0
CRACK LENGTH a [mm]

(b)

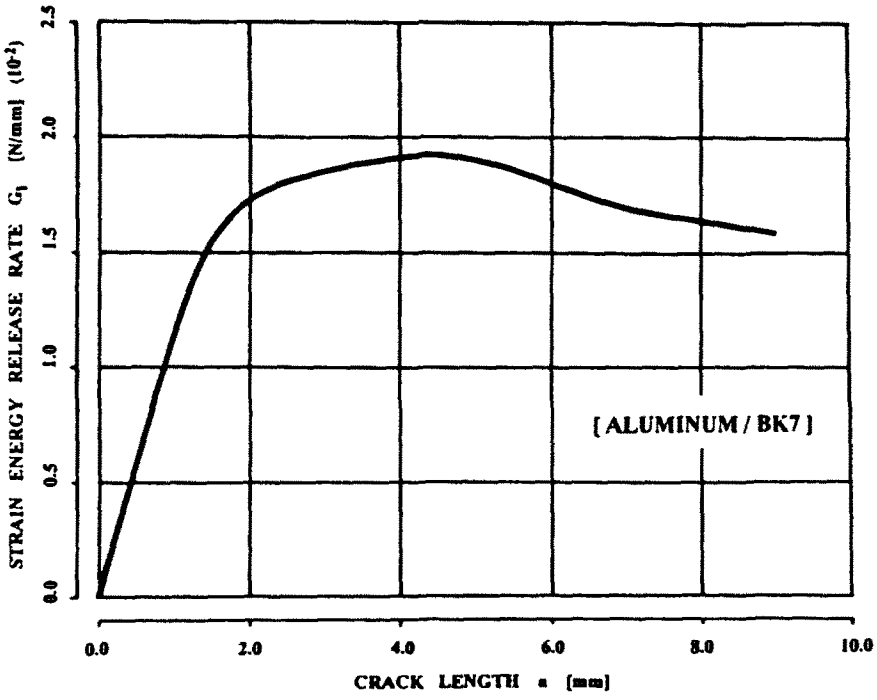

(c)

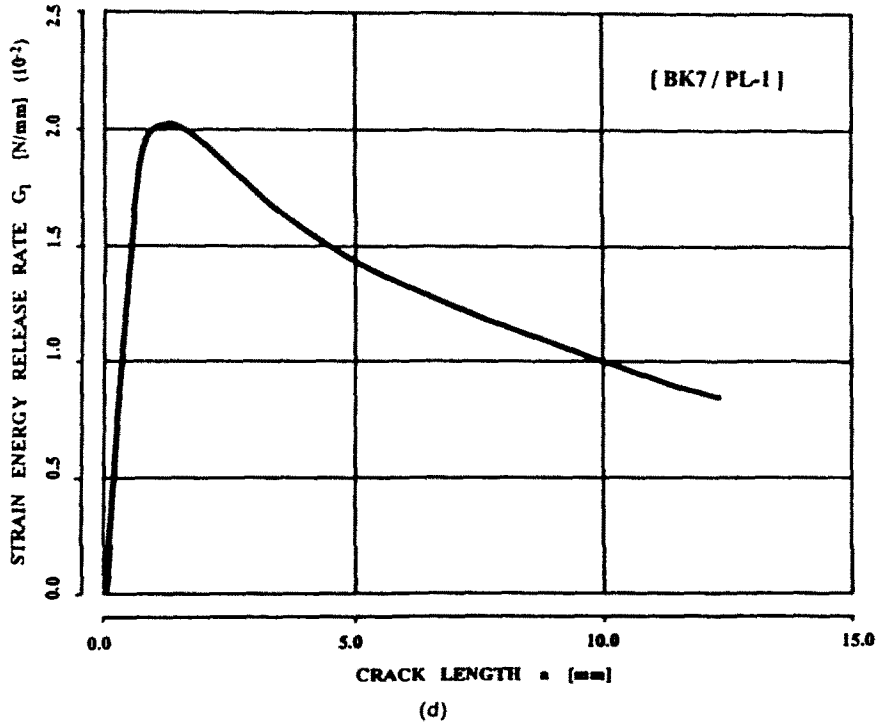

(d)

Fig. 7(a)–(d). Energy release rate $G = G_I$ as function of crack length a for different self-stressed two-phase composite structures.

composite structures subjected to uniform and nonuniform temperature loadings, respectively. Usually four to eight iterations have to be performed in order to get the new crack propagation direction. Figure 5a and b shows two examples of finite element meshes used for the crack path prediction described earlier. Further, an automatic control program was generated in order to evaluate energy release rates G_j ($j = I, II$) according to eqns (20) and (21) and to judge the iterations so that, after reaching the given tolerance, a new propagation step starts continuously. After execution of this computational program curved crack paths predicted numerically have been obtained. Figure 6a–e shows a comparison of numerically predicted crack paths with curvilinear thermal crack paths gained from associated cooling experiments for different shaped two-phase composite structures subjected to a uniform temperature distribution. The numerically and experimentally obtained crack paths show an excellent agreement.

3.3. *Determination of fracture mechanical data*

Figure 7a–d gives the energy release rate $G = G_I$ as a function of crack length a corresponding to the crack paths shown in Fig. 6a–d and calculated numerically according to formulae (20)–(22).

Finally, Fig. 8 gives a comparison of numerically and experimentally obtained stress intensity factors K_j ($j = I, II$) at the tip of a curvilinear thermal crack in a self-stressed Araldite B/ABS composite structure (geometrical parameters: $R = 75$ mm, $t = 5$ mm) subjected to a uniform temperature distribution $\Delta T = -40$ K. It can be seen that the quasistatic extension of this curved thermal crack occurs essentially under Mode I loading. Further, it should be mentioned that for self-stressed two-phase compounds with a cracked glassy segment, for instance for the compound structure Glass (SF11)/Aluminum, a photoelastic thermal crack analysis has been performed by using the image analysis of photoelastic fringes as well as the so-called multiplication method of isochromatic fringe loops. Moreover, a computer program for the determination of stress intensity factors K_j ($j = I, II$) was developed by consideration of the so-called multiparameter method (Ferber *et al.*, 1990). The comparison of the experimental results obtained from cooling experiments and the numerical results gained by associated finite element computations showed again a satisfying agreement.

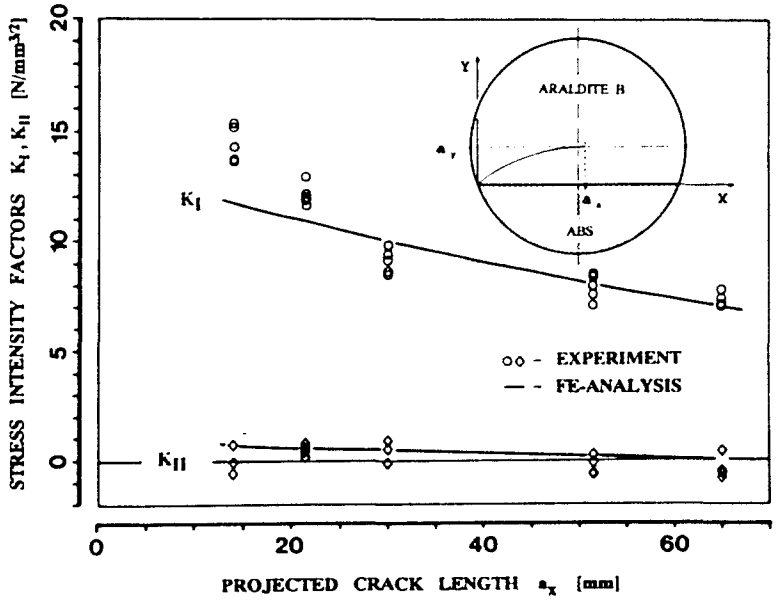

Fig. 8. Comparison of numerically and experimentally gained stress intensity factors K_j ($j = I, II$) at the tip of a curvilinear thermal crack in an Araldite B/ABS composite structure.

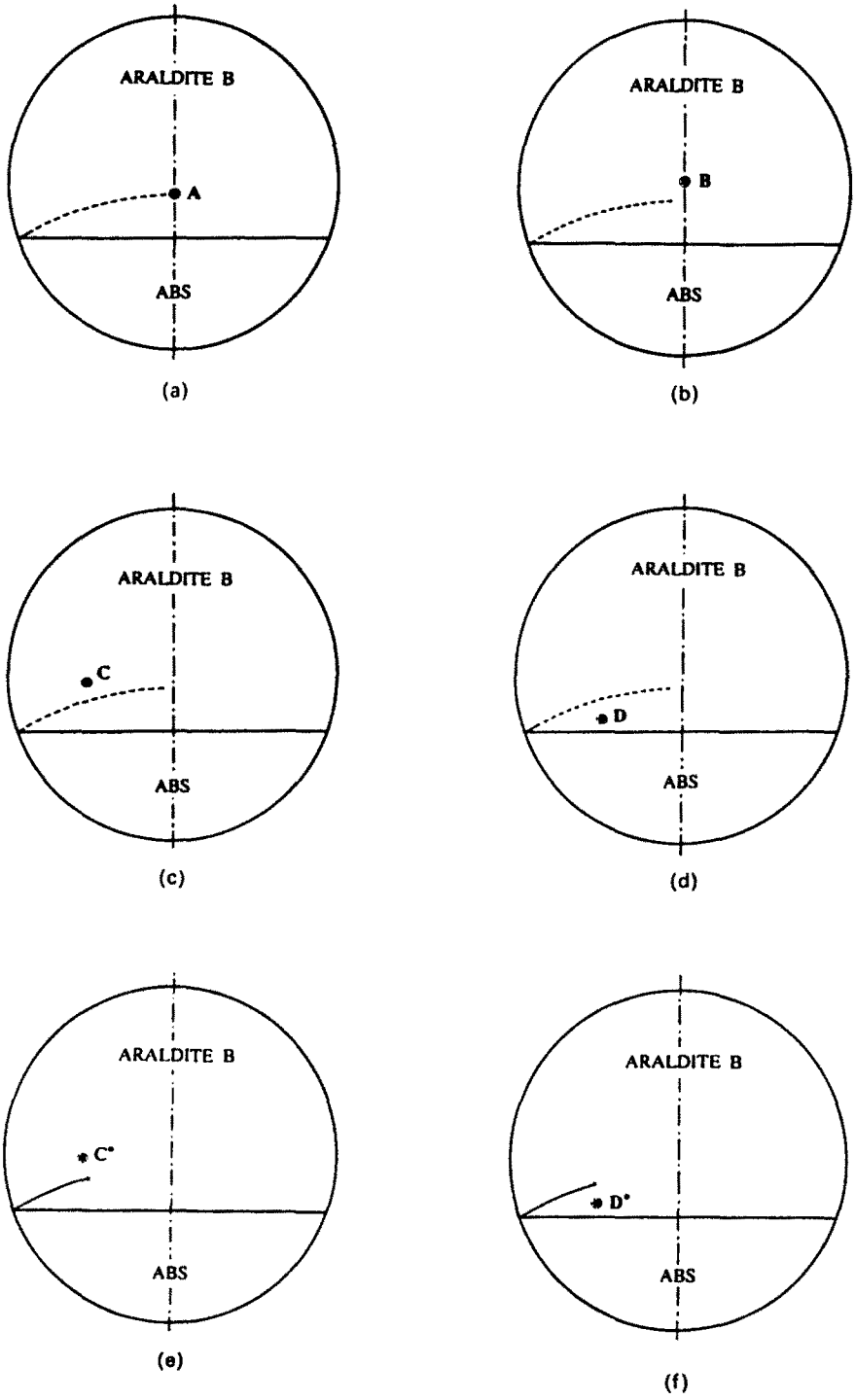

Fig. 9(a)–(f). Positions of the additional local temperature change in the cross-section of the composite structure Araldite B/ABS.

4. CRACK PATH PREDICTION AND CALCULATION OF STRESS INTENSITY FACTORS CONCERNING THERMAL CRACKS ARISING IN SELF-STRESSED TWO-PHASE COMPOUNDS SUBJECTED TO NONUNIFORM TEMPERATURE DISTRIBUTIONS

In this section cracked two-phase compounds are studied subjected to special non-uniform temperature distributions. Thereby the influence of very restricted local temperature changes on the thermal crack growth as well as on the values of the corresponding fracture mechanical data at the tips of curvilinear thermal cracks arising in self-stressed two-phase solids was investigated. Further, this non-uniform temperature distribution applied to these composite structures is composed in such a way that on the basis of a uniform temperature load applied to the whole cross-section of a two-phase compound additional local temperature changes $\Delta T^* \gtrless 0$ acting inside of a small circular region with a radius of $r^* \approx 1.2$ mm have to be added. The locations of these additional local temperature changes in the cross-section of a self-stressed composite structure (Araldite B/ABS) are shown in Fig. 9 with the following abbreviations:

H: homogeneous temperature distribution, $\Delta T = -40$ K;
A_Q, B_Q, C_Q, D_Q: additional temperature rise with $\Delta T^* = 100$ K in the vicinity of the points A, B, C, D before thermal crack initiation;
A_S, B_S, C_S, D_S: additional temperature drop with $\Delta T^* = -100$ K in the vicinity of the points A, B, C, D before thermal crack initiation;
C_Q^*, D_Q^*: additional temperature rise with $\Delta T^* = 100$ K in the vicinity of the points C^*, D^* after arrival of the thermal crack at these points;
C_S^*, D_S^*: additional temperature drop with $\Delta T^* = -100$ K in the vicinity of the points C^*, D^* after arrival of the thermal crack at these points.

All of these cases have been studied by appropriate finite element calculations by using the proposed crack growth criterion of Section 3 as well as Irwin's modified crack closure integral for the determination of fracture mechanical data. Figures 10–15 show the crack paths and corresponding stress intensity factors K_I at the tips of quasistatically extending thermal cracks due to the influence of a uniform temperature distribution as well as of additional local temperature changes ΔT^* acting in the cross-section of a thermally loaded composite structure Araldite B/ABS.

The influence of the local temperature changes ΔT^* either on the curvilinear thermal crack paths or on the stress intensity factors K_I at the corresponding crack tips can be observed in Figs 10–15. Because of the very restricted size of the regions of additional local temperature changes there arise only relatively small differences between the results of the uniform and nonuniform temperature distributions, respectively. Now from the numerical results shown in Figs 10–15 the following conclusions about the effects of additional local temperature changes ΔT^* in the cross-section of a self-stressed two-phase composite structure can be made.

(a) The closer the crack tip lies to a center of an additional local temperature change ΔT^*, the greater is the influence of this center on the thermal crack path as well as on the fracture mechanical data at the corresponding crack tip.

(b) If the center of an additional local temperature change lies just in the prospective thermal crack path obtained for a uniform temperature distribution, then the new crack path almost remains the same.

(c) If the center of an additional local temperature change lies outside of the prospective thermal crack path gained for a uniform temperature distribution, the new crack path shows the tendency to approach a center of local temperature rise whereas, there exists an inclination of the crack to bypass a center of local temperature drop.

(d) If the center of an additional local temperature change lies in a certain distance ahead of a thermal crack tip, either outside of or on the prospective crack path, then the corresponding fracture mechanical data at the crack tip will be increased in the case of an additional local temperature rise and will be decreased in the case of an additional local temperature drop. On the contrary, if the center of an additional local temperature change lies in a certain distance behind of a thermal crack tip, then the inverse effects occur concerning the fracture mechanical data.

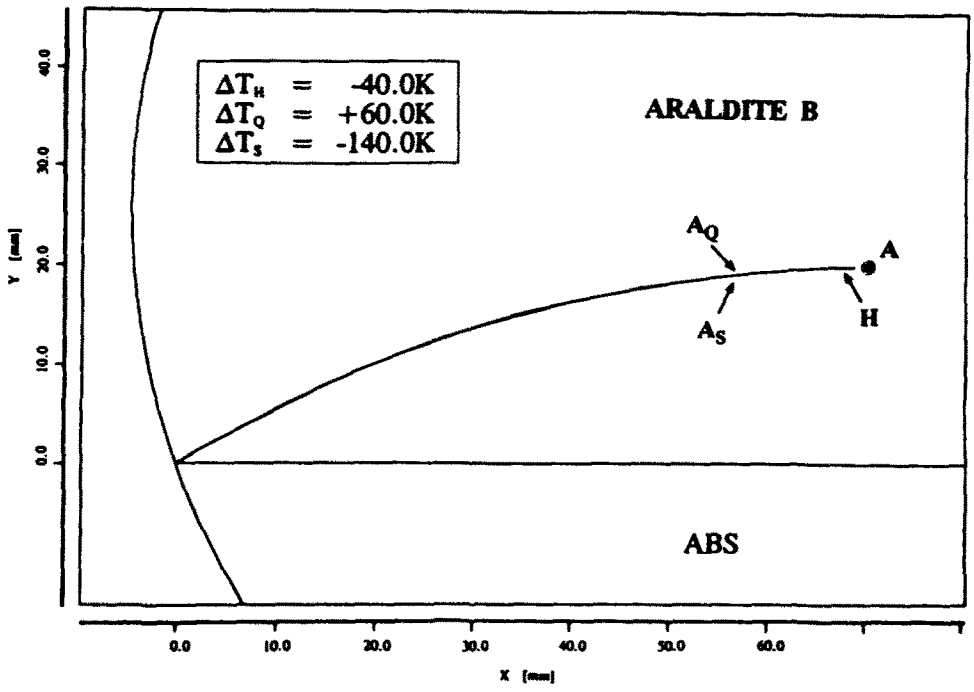

(a)

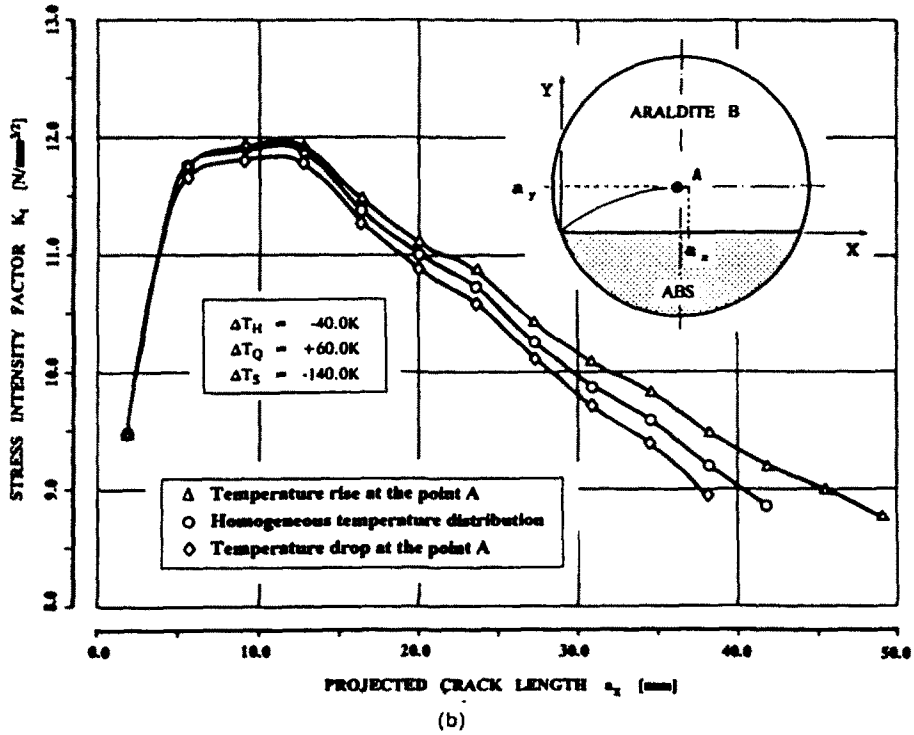

(b)

Fig. 10. Crack paths and stress intensity factors K_I in the cases of A_Q, A_S and H. (a) Crack paths. (b) K_I values.

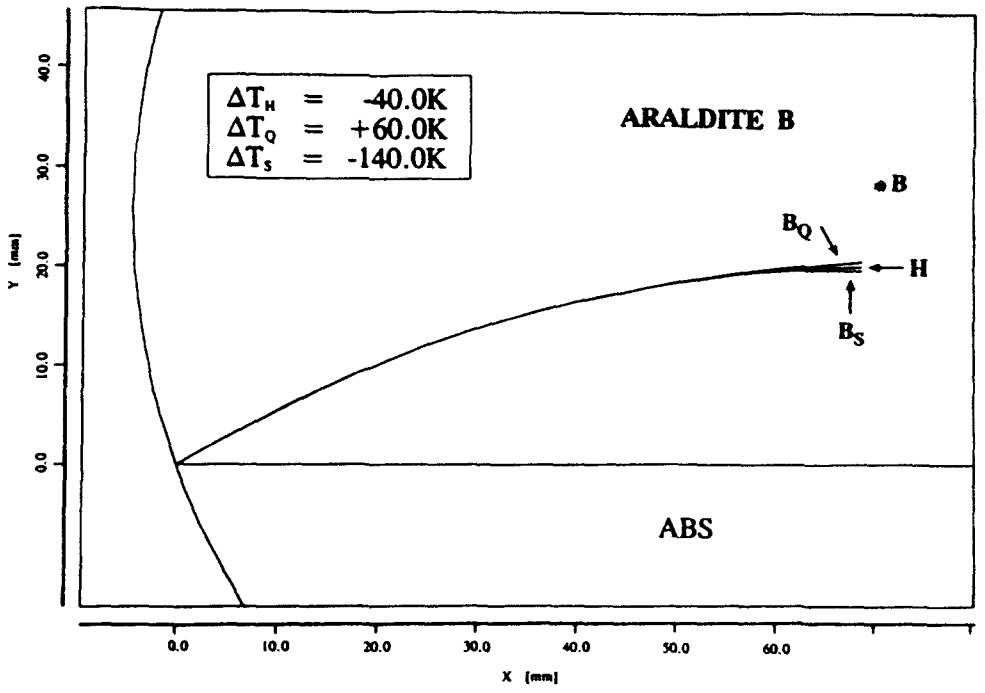

(a)

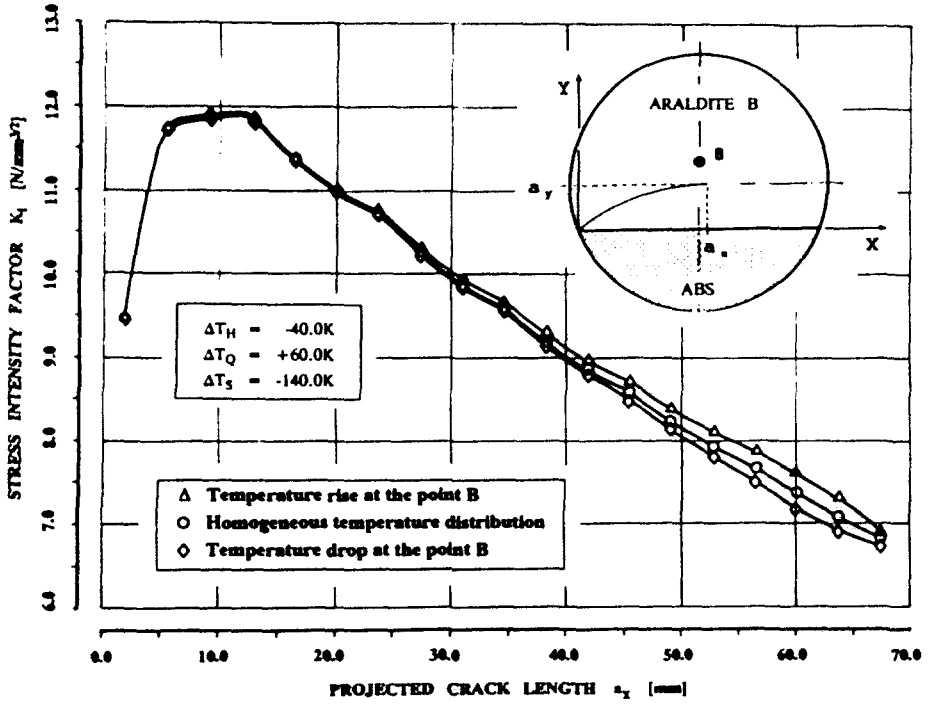

(b)

Fig. 11. Crack paths and stress intensity factors K_I in the cases of B_Q, B_S and H. (a) Crack paths. (b) K_I values.

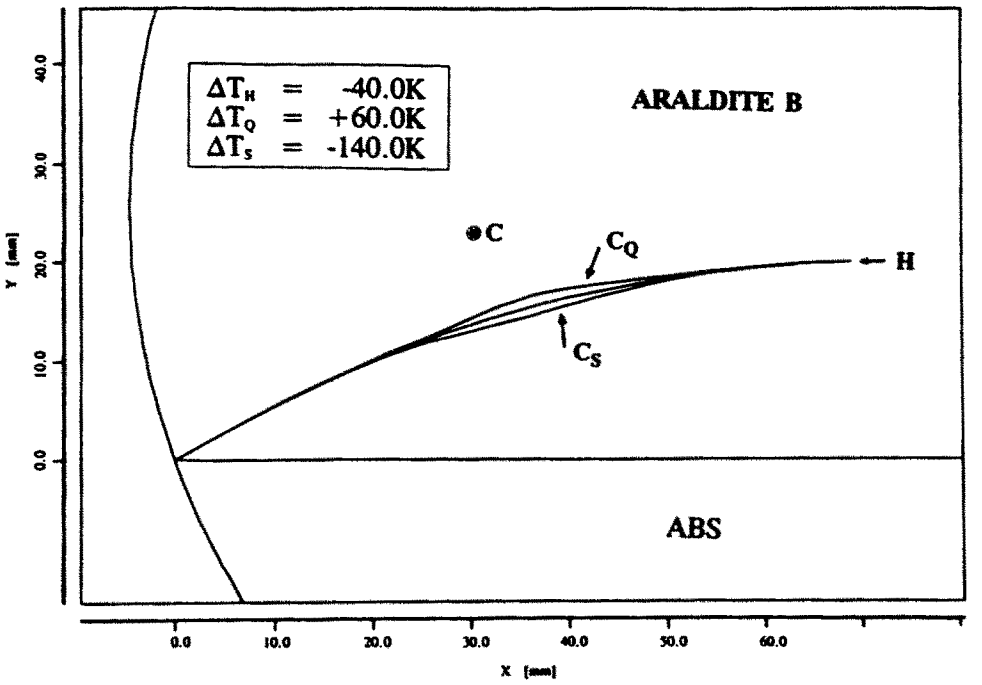

(a)

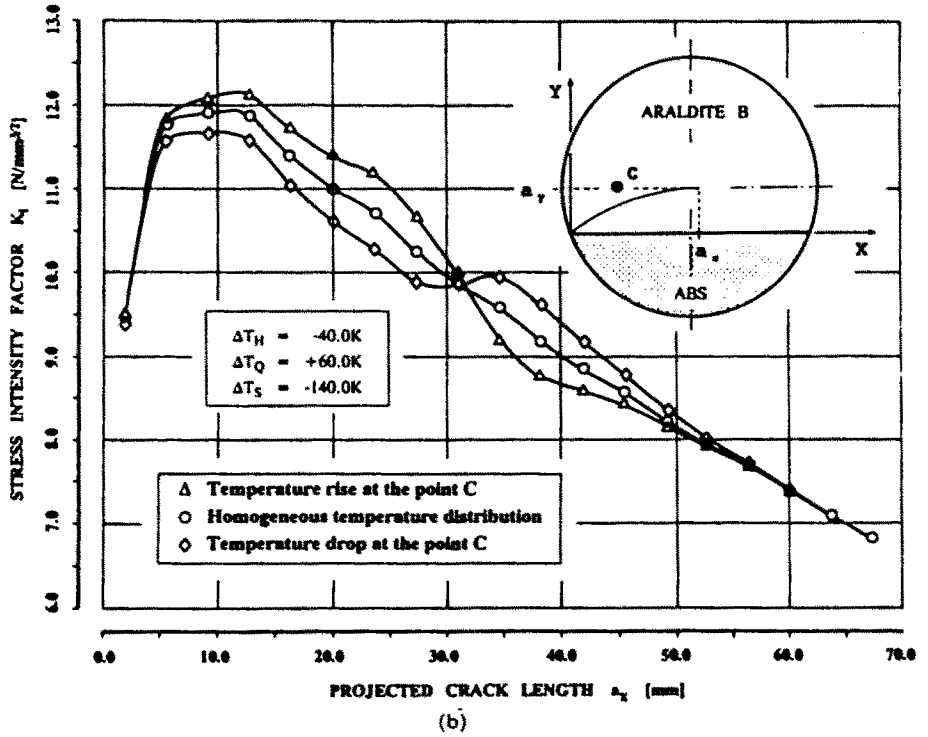

(b)

Fig. 12. Crack paths and stress intensity factors K_I in the cases of C_Q, C_S and H. (a) Crack paths. (b) K_I values.

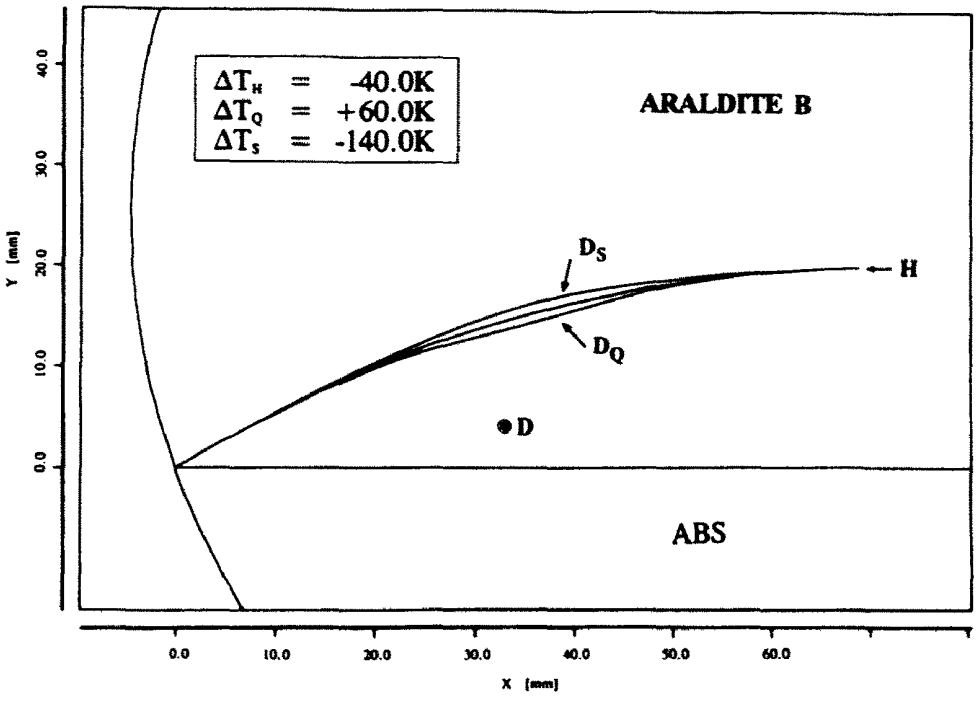

(a)

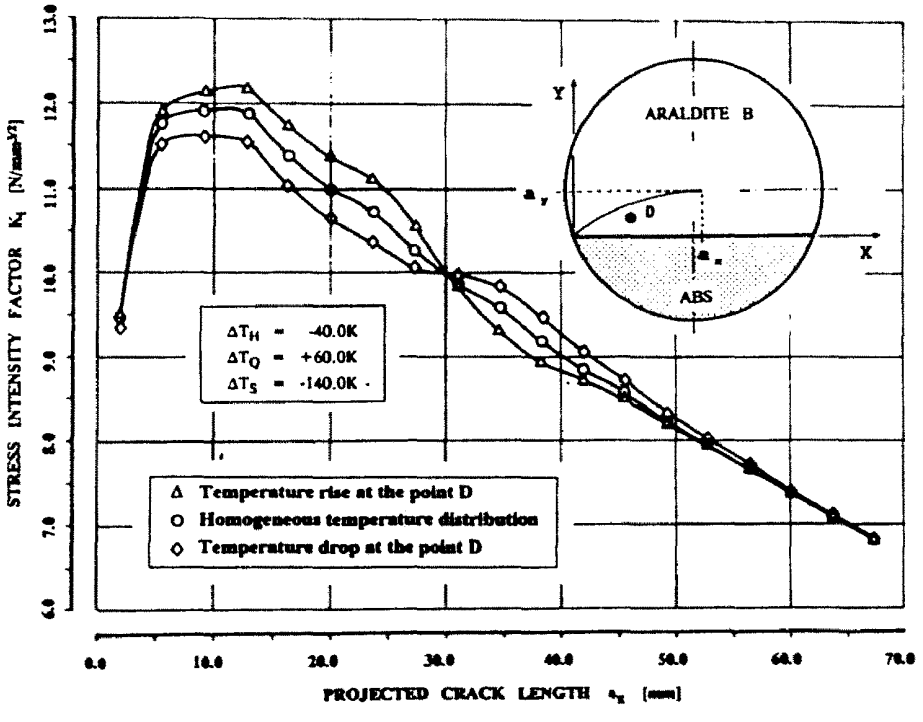

(b)

Fig. 13. Crack paths and stress intensity factors K_I in the cases of D_Q, D_S and H. (a) Crack paths. (b) K_I values.

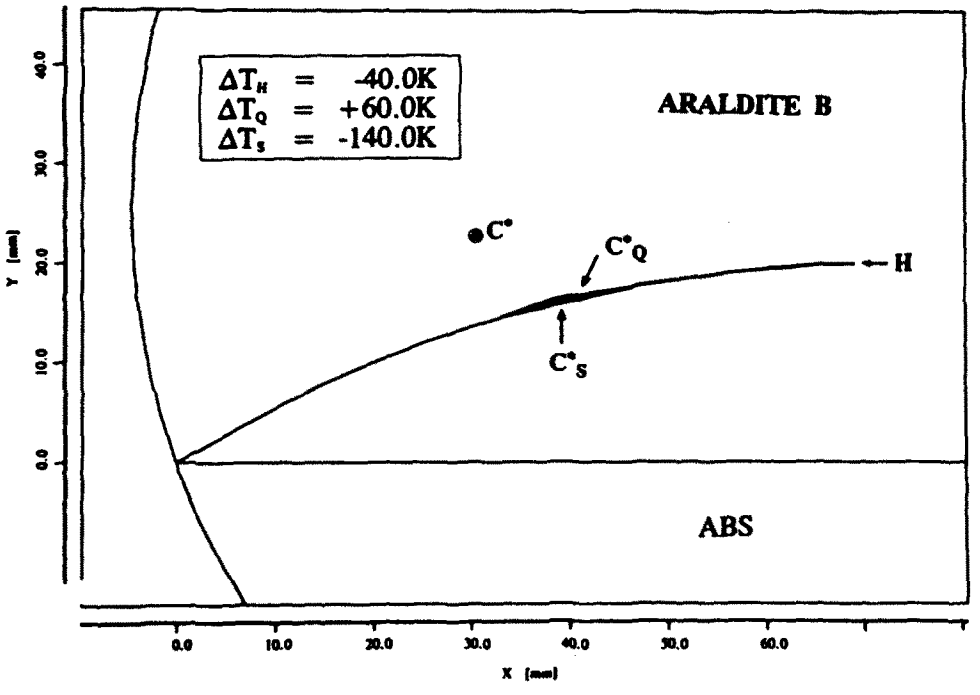

(a)

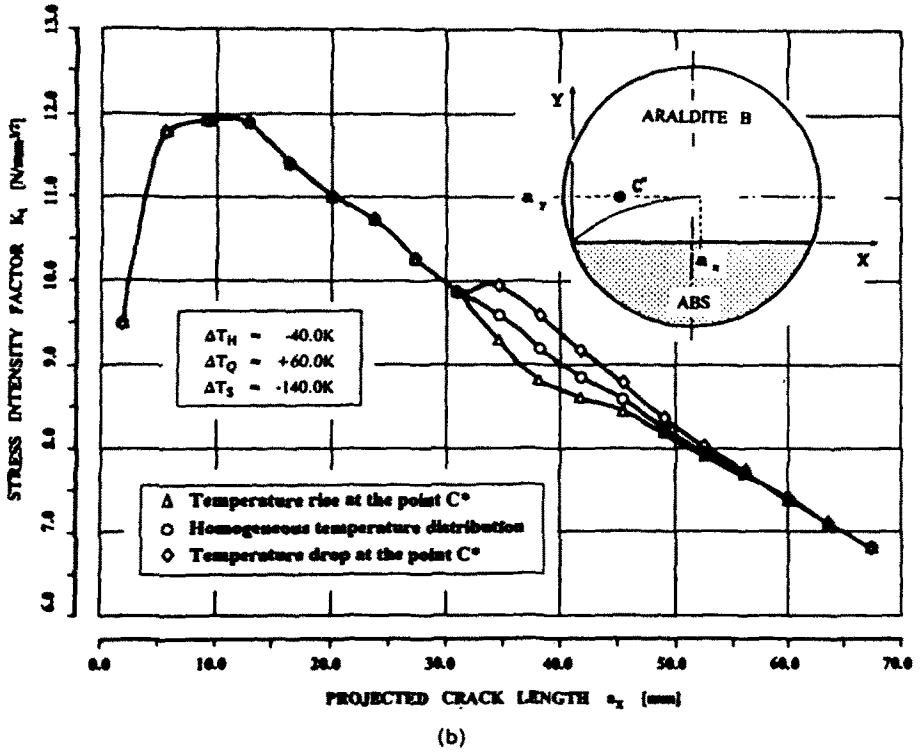

(b)

Fig. 14. Crack paths and stress intensity factors K_I in the cases of C_Q^*, C_S^* and H. (a) Crack paths. (b) K_I values.

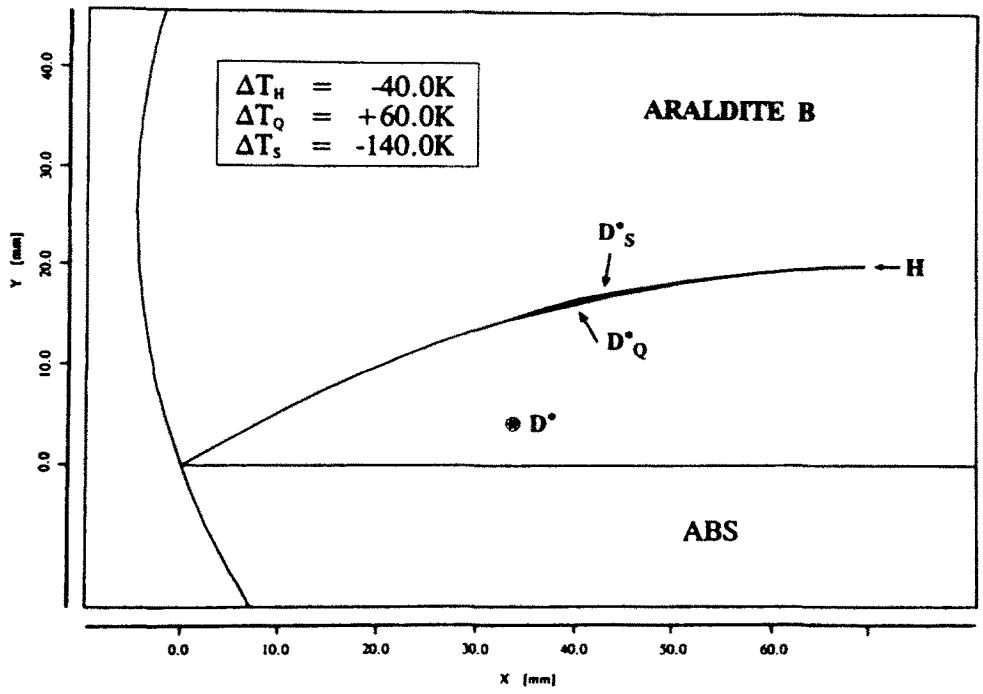

(a)

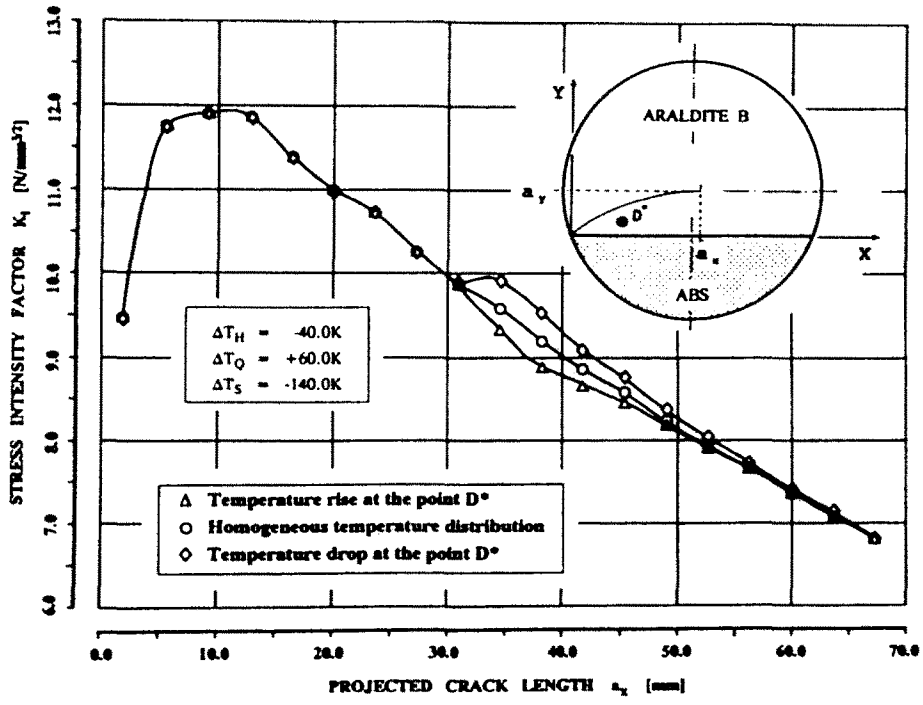

(b)

Fig. 15. Crack paths and stress intensity factors K_I in the cases of D_Q^*, D_S^* and H. (a) Crack paths. (b) K_I values.

5. CONCLUSIONS

The crack path prediction of thermal cracks in self-stressed two-phase composite structures subjected to uniform and non-uniform temperature distributions, respectively, has been investigated by using the finite element method as well as by applying an appropriate crack growth criterion. The latter is based upon the numerical calculation of the energy release rates at the corresponding thermal crack tips and predicts a further crack extension in the direction in which G_{II} equals zero. A series of different cracked two-phase composite structures subjected to uniform as well as nonuniform temperature distributions, respectively, has been studied by using the crack growth criterion mentioned above. Thereby thermal cracks always arise on the side of Max $[\alpha^{(J)}\Delta T^{(J)}, J = I, II]$ in the corresponding self-stressed two-phase solids starting from the intersection point of the material interface Γ with the external surface S. A comparison of the numerically obtained results in case of the existence of a uniform temperature distribution in the cross-sections of two-phase compounds for both the thermal crack paths and the corresponding fracture mechanical data at the crack tips with the experimental results gained from associated cooling experiments showed a good agreement.

In addition, the influence of very restricted local temperature changes ΔT^* onto the prospective thermal crack paths has been studied by means of the crack growth criterion already mentioned as well as by using the finite element method. Thereby some remarkable effects of interference between the centers of local temperature changes located in the vicinity of the tips of thermal cracks and their further crack paths could be stated. This interference is also observable concerning the corresponding fracture mechanical parameters at the tips of the arising curvilinear thermal cracks.

Acknowledgement—The financial support of the German Research Association (DFG) is gratefully acknowledged by the authors.

REFERENCES

Bergkvist, H. and Guex, L. (1979). Curved crack propagation. *Int. J. Fract.* **15**, 429–441.
Blauel, H. (1970). Ph.D. dissertation. Freiburg University.
Bregman, A. M. and Kassir, M. K. (1974). Thermal fracture of bonded dissimilar media containing a penny-shaped crack. *Int. J. Fract.* **10**, 87–98.
Brown, E. J. and Erdogan, F. (1968). Thermal stresses in bounded materials containing cuts on the interface. *Int. J. Engng Sci.* **6**, 517–529.
Cotterell, B. and Rice, J. R. (1980). Slightly curved or kinked cracks. *Int. J. Fract.* **16**, 155–169.
England, A. (1966). An arc crack around a circular elastic inclusion. *J. Appl. Mech.* **33**, 637–640.
Erdogan, F. and Sih, G. C. (1963). On the crack extension in plates under plane loading and transverse shear. *J. Basic Engng* **85**, 519–527.
Ferber, F., Hinz, O. and Herrmann, K. P. (1990). Bruchmechanische Analyse von Eigenspannungsrißproblemen in Verbundgläsern mittels spannungsoptischer Methoden. *VDI-Berichte* **815**, 459–470.
Grebner, H. (1983). Ph.D. dissertation. Paderborn University.
Herrmann, K. P. (1983). Curved thermal crack growth in the interfaces of a unidirectional Carbon–Aluminum composite. In *Mechanics of Composite Materials, Recent Advances* (Edited by Z. Hashin and C. T. Herakovich), pp. 383–397. Pergamon Press, New York.
Herrmann, K. P. (1987). Thermal crack growth in self-stressed glassy compounds. In *Fracture of Non-Metallic Materials* (Edited by K. P. Herrmann and L. H. Larsson), pp. 181–205. Reidel, Dordrecht.
Herrmann, K. P. and Dong, M. (1990). Bruchmechanische Untersuchungen zum Mixed-Mode Problem sowie zur Rißwegvorhersage in Zweikomponentenmaterialien. *ZAMM* **70**, T292–294.
Herrmann, K. P., Dong, M. and Hinz, O. (1991). Wärmespannungsrisse in Zweiphasenmedien unter inhomogener Temperaturverteilung. *ZAMM* **71**, T283–287.
Herrmann, K. P. and Ferber, F. (1989). Elementary failure mechanisms in thermally stressed models of fiber reinforced composites. In *Brittle Matrix Composites* (Edited by A. M. Brandt and I. H. Marshall), Vol. 2, pp. 1–19. Elsevier, London and New York.
Herrmann, K. P. and Grebner, H. (1982). Curved thermal crack growth in a bounded brittle two-phase solid. *Int. J. Fract.* **19**, R69–R74.
Herrmann, K. P. and Grebner, H. (1984a). Curved thermal crack growth in nonhomogeneous materials with different shaped external boundaries. I. Theoretical results. II. Experimental results. *Theor. Appl. Fract. Mech.* **2**, 133–155.
Herrmann, K. P. and Grebner, H. (1984b). Slow thermal crack growth in thermally loaded two-phase composite structures containing inner stress concentrators. In *Life Assessment of Dynamically Loaded Materials and Structures* (Edited by L. Faria), pp. 691–700. Lissabon.
Herrmann, K. P. and Grebner, H. (1985). Quasistatic thermal crack extension in the interfaces of bounded self-stressed multiphase compounds. *Theor. Appl. Fract. Mech.* **4**, 127–135.

Herrmann, K. P. and Strathmeier, U. (1983). Quasistatic extension of an interface crack. In *Fracture and the Role of Microstructure* (Edited by K. L. Maurer and F. E. Matzer), pp. 199–206. EMAS, Warley.

Hieke, M. (1960). Die Rißentstehung in Glasscheiben unter Eigenspannungen. *Z. Naturforsch.* **15a**, 543–546.

Hieke, M. and Loges, F. (1966). Des Zerreißen von Gläsern unter dem Einfluß definierter Eigenspannungsquellen. *Z. Angew. Phys.* **22**, 14–19.

Hussain, M. A., Pu, S. L. and Underwood, I. (1972). Strain energy release rate for a crack under combined Mode I and Mode II. *ASTM STP* **560**, 2–28.

Karihaloo, B. L. and Nemat-Nasser, S. (1981). Thermally induced crack curving in brittle solids. In *Analytical and Experimental Fracture Mechanics* (Edited by G. C. Sih and M. Mirabile), pp. 265–272. Sijthoff & Noordhoff, Alphen aan den Rijn.

Muskhelishvili, N. I. (1971). *Einige Grundaufgaben zur mathematischen Elastizitätstheorie*. Fachbuchverlag, Leipzig.

Nemat-Nasser, S. (1980). On stability of the growth of intersecting cracks, and crack kinking and curving in brittle solids. In *Numerical Methods in Fracture Mechanics* (Edited by D. R. J. Owen and A. R. Luxmoore), pp. 687–706. Pineridge Press, Swansea.

Palaniswamy, K. and Knauss, W. G. (1978). On the problem of crack extension in brittle solids under general loading. *Mechanics Today* (Edited by S. Nemat-Nasser), Vol. 4, pp. 87–148. Pergamon Press, New York.

Piva, A. and Viola, E. (1980). Biaxial load effects on a crack between dissimilar media. *Engng Fract. Mech.* **13**, 143–174.

Rybicki, E. F. and Kanninen, M. F. (1977). A finite element calculation of stress intensity factors by a modified crack closure integral. *Engng Fract. Mech.* **9**, 931–938.

Sih, G. C. (1973). A special theory of crack propagation. In *Mechanics of Fracture* (Edited by G. C. Sih), Vol. 1, XXI–XLV. Noordhoff, Leyden.

Sih, G. C. (1974). Strain-energy-density factor applied to mixed-mode crack problems. *Int. J. Fract.* **10**, 305–321.

Srivastava, K. N., Palaiya, R. M. and Choudhary, A. (1977). Thermal stresses in an elastic layer containing a penny-shaped crack and bonded to dissimilar half-spaces. *Int. J. Fract.* **13**, 27–38.

Strifors, H. C. (1974). A generalized force measure of conditions at crack tips. *Int. J. Solids Structures* **10**, 1389–1404.

Toya, M. (1974). A crack along the interface of a circular inclusion embedded in an infinite solid. *J. Mech. Phys. Solids* **22**, 325–348.